Наносистеми, наноматеріали, нанотехнології
Nanosistemi, Nanomateriali, Nanotehnologii
2026, т. 24, № 1, сс. 105–113
https://doi.org/10.15407/nnn.24.01.0105

PACS numbers: 68.37.Hk, 73.61.Ga, 78.20.Ci, 78.66.Hf, 78.67.Bf, 78.67.Pt

Structural, Optical, and Electrical Properties of Nano-Zinc Sulphide at 250°C

Sabah S. Hamdi

College of Computer Science and Mathematics,
Physics Department,
Tikrit University,
34001 Tikrit, Iraq

The thin films of zinc sulphide (ZnS) with nanograins are produced on (glass) substrates at 250°C using the spray-pyrolysis deposition technique (SPDT). The films have a polycrystalline cubic structure with preferred orientation along (111) direction of growth. The optical characteristics of the thin ZnS film indicate a direct optical energy gap of 3.320 eV. The film displays a thickness of 250.25 nm with grain sizes ranging from 9.76 nm to 11.46 nm. For approximate values, the measurements are done with the use of a computer simulation tool 'Hebal Optic'. It is also observed for all the films that there is an inverse proportional change in resistance to temperature and that the formed films have two activation energies.

Тонкі плівки сульфіду Цинку (ZnS) з нанозернами було одержано на скляних підкладинках за 250°C за допомогою методу осадження розпорошувальною піролізою. Плівки мали полікристалічну кубічну структуру з переважною орієнтацією вздовж напрямку росту (111). Оптичні характеристики тонкої плівки ZnS вказували на ширину прямої оптичної забороненої енергетичної зони у 3,320 еВ. Плівка мала товщину у 250,25 нм із розмірами зерен від 9,76 нм до 11,46 нм. Для одержання приблизних значень міряння виконувалися за допомогою засобу комп'ютерного моделювання «Hebal Optic». Також було відзначено, що для всіх плівок є обернено пропорційна зміна опору з температурою та що утворені плівки мають дві енергії активації.

Key words: software 'Hebal Optic', nano-ZnS, thiourea, energy gap, spray-pyrolysis deposition technique.

Ключові слова: програмні засоби «Hebal Optic», нано-ZnS, тіосечовина, заборонена енергетична зона, метод розпорошувальної піролізи.

(Received 6 July, 2024; in revised form, 17 September, 2024)

1. INTRODUCTION

Zinc sulphide (ZnS), also referred to as sphalerite, is a chemical compound having the chemical formula ZnS. Its name suggests a lack of similarity with other minerals. ZnS is a transparent, semiconducting, and yellow salt. The dissolution of ZnS is limited because to its low sublimation; hence, it is soluble in acids but not in water. Additionally, it exhibits low toxicity [1]. Because of its broad energy gap, ZnS is an excellent material for luminescence, which may be achieved in the almost visible range with appropriate grafting. ZnS is now considered as one of the best materials for diodes among multi-buffer layers. Compared with CdSe or CdS, benefits of the ZnS include its environmentally safe handling and nontoxic, and moreover, its ability to provide better lattice matching to CIGS absorbers with energy gaps ranging from 1.30 to 1050 eV, when compared to CdS, which transmits photons with higher energy and boosts light absorption in the absorber layer [2]. ZnS has many applications according to the physical and chemical properties for it, including field effect transistors. ZnS has two phase compositions: one is the cubic zinc blende phase, the most appropriate phase at 300 K, which may transform into the hexagonal phase, upon heating to 1298 K under atmospheric pressure; while, the other compound belongs to the wurtzite-type phase of hexagonal system, which is the most preferred phase for its optical optimum, ZnS is consistently utilized in blue light-emitting lasers' diodes, and antireflective and corrosion coatings. It is always used to create television and x-ray screens [3].

2. EXPERIMENTAL PART

Nanosize thin ZnS films are produced using an aqueous solution of zinc nitrate (a white powdered material, which is dissolved more rapidly in water than in other liquids, with a molecular weight of 297.364 g/mole and a purity of 99.96%) and thiourea (C.S. $(NH_2)_2$). The colure is a white powder rapidly soluble in water. An initial solution, weighing 76.614 g/mole and having a purity of 98%, was obtained by dissolving 1.480 g of zinc nitrate in 0.1 L of distilled water at room temperature. A second solvent, with a concentration of 0.01 M, was also made at room temperature. The solvent were mixed using a magnetic mixer to dissolve completely thiourea (0.076 g) in 100 mL of distilled water. The solvent was placed on a

magnetic mixer for 10 minutes until homogenous and free of plankton. The two solvent were then mixed in an equal volume ratio (1:1); for getting a homogeneous solution, the solution was stirred with a magnetic stirrer for an additional 10 minutes.

Thin ZnS films are formed, when the solution is deposited onto a glass substrate using a chemical decomposition process. Thermochemical spraying technology was chosen to appropriate for creating oxide and sulphate materials and is inexpensive according to the cheap cost of the equipment required to generate these films. The film can be created by combining two components or by combining materials with various melting points. The film is formed using normal conditions. The prepared solution is applied to the glass substrate at 250°C; the average distance from the sprayer (nozzle) to the glass substrate is of 28 cm, as a larger distance would cause the material to evaporate before reaching the substrate.

The glass substrate with a thickness of 0.1 cm is covered with a thin layer. The properties of the resulting film can be affected by the presence of impurities; so, the glass substrate is thoroughly cleaned before spraying. The substrate is cleaned after cutting it into small squares of 2.5 cm×2.5 cm. To remove plankton, the substrate is first rinsed with water. The substrate is then incubated in a glass flask with 99.99%-pure acetone for 10 minutes. The substrate is then incubated in another container with 99%-pure ethanol for 10 minutes. Finally, to remove any residual acetone and ethanol, the substrate (glass) was put in a flask containing only distilled water and let to stand for 15 minutes; to clean the glass lens, the glass substrate is finally wiped dry with a cloth. At 250°C, a thin layer of ZnS was deposited on the glass substrate.

3. RESULTS AND DISCUSSION

3.1. Structure

ZnS was prepared on a substrate (glass) at 250°C; then, it was annealed at 300°C for 30 min. XRD data showed that the system was cubic with (111) being the main growth direction. In Figure 1, angle $2\theta \cong 27.55°$, 47.87°, 56.39° corresponds to (220), (311) and (111) in sequence [4, 5]. The peak positions of ZnS in XRD were compared with ICDD 00-001-0792 and the structural characteristics of the standard peaks (Table 1).

Table 1 shows how close they are to each other. In addition, we observed that with increasing base temperature, the peak intensity of the ZnS nanocrystal-size film increased and the full width at half-maximum (*FWHM*) curve decreased. This supports the increase in the percentage of crystallization, as the increase in peak height

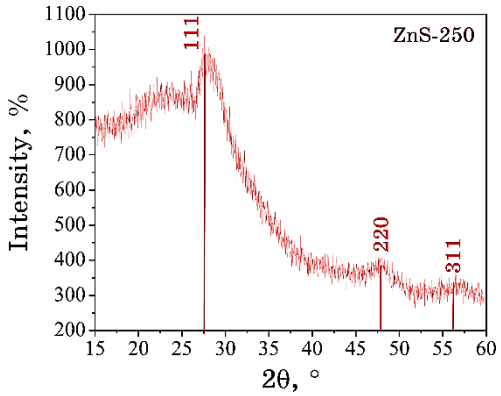

Fig. 1. XRD for ZnS at substrate temperature of 250°C.

TABLE 1. Structural parameters of ZnS at 250°C.

Sample	2θ	*hkl*	d_{hkl}, Å	*FWHM*	*D*, nm
ZnS-250°C	27.55	(111)	3.12	0.8659	9.87
	47.87	(220)	1.91	0.8755	9.76
	56.39	(311)	1.63	0.7456	11.46

Fig. 2. FE-SEM for thin ZnS-250°C film.

indicates a decrease in crystal defects and an increase in crystallization [6]. The average grain size of ZnS was within the range of 9.76 nm–11.46 nm, when computed using Eq. (1):

$$D_{ave} = \frac{0.9}{\beta \cos\theta} \tag{1}$$

($\lambda = 1.5406$ Å is x-ray wavelength (K_α-line); β is XRD 'full width at half-maximum' [in radians]; θ is Bragg's diffraction angle) [7].

When observing the morphology of the film surface using a scanning electron microscope (FE-SEM), as in Fig. 2, the ZnS-250°C film consists of orderly arranged nanosheets, which adhere to each other. This is the result of increasing heat to stimulate grain growth and alignment. As can be seen in Fig. 2, the particles have this shape, which is related to Refs. [4–6]. The thickness of the film was calculated using a computer simulation tool called 'Hebal Optic'. Based on the permeability value, the film thickness was determined to be approximately of 250.25 nm. The film was found to have a thickness of 250.25 nm.

3.2. Optical Properties

To calculate the absorption coefficients, we used equation

$$\alpha h\nu = \beta\left(h\nu - E_g\right)^r \tag{2}$$

(β is a constant, α is the absorption coefficient, $h\nu$ represents the energy of photon, E_g is optical energy gap, and $r = 1/2$ is allowed direct transition) and Fig. 3, which depicts the absorption spectrum ($A = \log(T/d)$, d is thickness of the sample, T is transmission) as a function of wavelength. The findings indicated that, when the substrate temperature increases, the generated thin-film absorbency improves, indicating enhanced crystallization (increase in crystal size).

Figure 4 depicts how the absorption coefficient varies with incident photon energy. The results indicated that the absorption coefficient of thin ZnS films developed on a glass substrate increased with photon energy. The maximum absorption was seen at 320 nm,

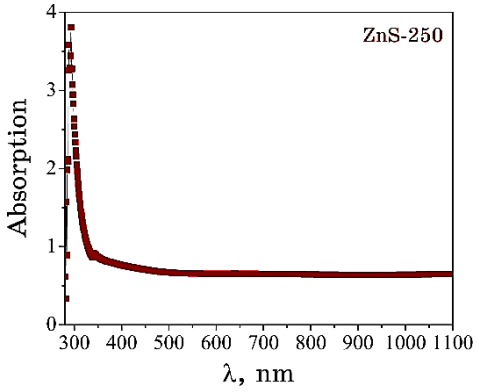

Fig. 3. The absorption of thin ZnS-250°C films.

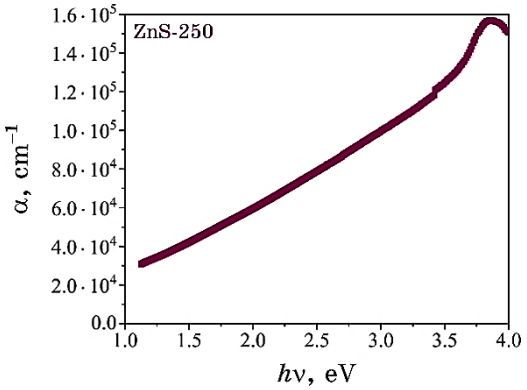

Fig. 4. The absorption coefficient of thin ZnS-250°C films.

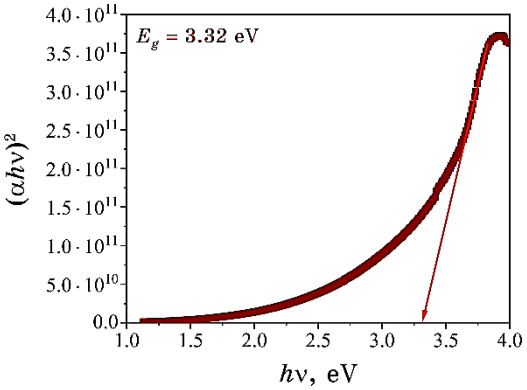

Fig. 5. Tauc plot for thin ZnS-250°C films.

with the highest values occurring at high photon energy ranging from 4 to 4.3 eV. This indicates that the absorption occurs within this specific frequency range, which encompasses the optical absorption edge.

The probability of electronic transitions occurring between the conduction and valence bands aligns with the results of empirical investigations [8, 9, 10]. The difference between the valence and conduction bands was calculated using the energy-gap value, which may be used to evaluate a material's electrical, thermal, and electronic properties. Equation (2) [11] demonstrates the application of the Tauc equation in computing the direct energy gap. Given that the transitions are permitted to be of the direct kind, characterized by a value of ($r = 1/2$), draw the link for tangent $(\alpha h\nu)^2$ and the incident photons' energy, then extend the curve straight portion to determine the point, where it crosses (where $(\alpha h\nu)^2 = 0$), represent

the optical energy gap.

In Figure 5, the band gap of the films was observed for ZnS; it has an optical energy gap of 3.32 eV at 250°C, which is nearly in line with the findings of Refs. [12, 13].

3.3. Electrical Properties

Figure 6 illustrates the link between inverse temperature and conductivity. The conductivity increases, when temperature increases from 40°C to 180°C, indicating that the layers are semiconductors. With increasing temperature, conductivity increases, while activation energy decreases. The underlying cause could be large particle sizes and excellent crystallization. Grain-boundary scattering has a general effect on charge-carrier mobility and film crystallinity. In our situation, grain expansion caused by the charge-carrier transport mechanism reduced grain-boundary scattering [14, 15]. To evaluate electrical conductivity, we use the given equation:

$$\sigma = \sigma_0 \exp\left(-\frac{E_a}{k_B T}\right) \tag{3}$$

(σ_0 is temperature-independent constant, E_a is activation energy for conduction, k_B is Boltzmann's constant, and here, T is a temperature [K]).

The conductivity and activation energy are shown in Table 2.

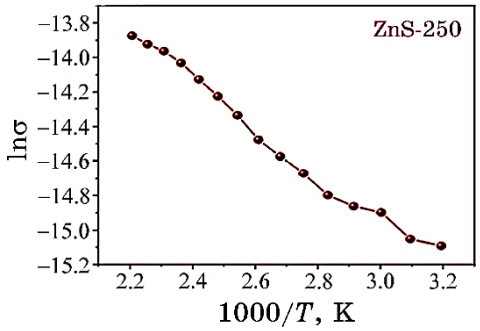

Fig. 6. Energy gap from electrical conductivity of ZnS-250°C films.

TABLE 2. The activation energy and optical energy gap.

Sample	E_{a1} (313–363 K)	E_{a2} (363–453 K)	E_a
ZnS-250°C	0.903 eV	1.833 eV	3.32 eV

Energy gap can be computed using the linear relationship, as illustrated in Fig. 6.

For the thin ZnS films, the presence of two linked zones is the reason for the alteration in the conduction mechanism. The temperature in the first zone is low (313–363 K), whereas the second zone is greater (363–453 K) [16].

4. CONCLUSION

The thin ZnS films were formed on a glass substrate using spray-pyrolysis deposition technique. The x-ray diffraction (XRD) study of this thin film revealed a 'full width at half maximum' (*FWHM*) value of 0.141°. This indicates that the crystallinity of the films can be enhanced by increasing the temperatures of the glass substrate. It was also shown that all films had a cubic crystal structure with a favourite (111) orientation. An increase in substrate temperature resulted in enhanced crystalline quality of the films, accompanied by a growth in grain sizes of thin film from 9.760 nm to 11.460 nm. A comprehensive analysis of the morphological, optical, and structural characteristics of the films was carried out using the computer program 'Hebal Optic' of simulation. The findings indicated an energy gap of 3.32 eV as well as nanoscale branching dendritic formations. As a result, it has semiconductor properties, which are important in electronic devices and solar cell manufacture.

ACKNOWLEDGEMENTS

Authors would like to thank the University of Tikrit, College of Education, Physics Department, management and staff for the support during the experimental-work stage.

REFERENCES

1. N. Imam and M. B. Mohamed, *Superlattices and Microstructures*, **73**: 203 (2014); https://doi.org/10.1016/j.spmi.2014.05.026
2. W. K. Bae, J. Kwak, J. W. Park, K. Char, C. Lee, and S. Lee, *Advanced Materials*, **21**, No. 17: 1690 (2009); https://doi.org/10.1002/adma.200801908
3. Hanaa I. Mohammed, Iman H. Khdayer, and Iqbal S. Naji, *AIP Conference Proceedings*, **2372**, No. 1: 090005 (2021); https://doi.org/10.1063/5.0068737
4. Jiaguo Huang and Kanyi Pu, *Chem. Int. Ed. Engl.*, **59**: 11717 (2020); https://doi.org/10.1002/anie.202001783
5. W. Daranfed, M. S. Aida, A. Hafdallah, and H. Lekiket, *Thin Solid Films*,

518, Iss. 4: 10821084 (2009); https://doi.org/10.1016/j.tsf.2009.03.227
6. J. Ady, S. F. Umroati, S. Meliana, S. D. A. Ariska, and D. I. Rudyardjo, *Nanosistemi, Nanomateriali, Nanotehnologii*, **19**, Iss. 3: 585 (2021); https://doi.org/10.15407/nnn.19.03.585
7. A. Ateş, M. Kundakçı, A. Astam, and M. Yıldırım, *Physica E: Low-dimensional Systems and Nanostructures*, **40**, Iss. 8: 2709 (2008); https://doi.org/10.1016/j.physe.2007.12.010
8. S. Ilican, Y. Caglar, M. Caglar, and F. Yakuphanoglu, *Physica E: Low-dimensional Systems and Nanostructures*, **35**, Iss. 1: 131 (2006); https://doi.org/10.1016/j.physe.2006.07.009
9. Z. Zhao, M. Liu, K. Yang, C. Xu, Y. Guan, X. Ma, and F. Zhang, *Advanced Functional Materials*, **31**, Iss. 43: 2106009 (2021); https://doi.org/10.1002/adfm.202106009
10. N. P. Huse, A. S. Dive, K. P. Guttu, and R. Sharma, *Mater. Sci. Semicond. Proc.*, **67**: 62 (2017); https://doi.org/10.1016/j.mssp.2017.05.010
11. K. Priya, V. K. Ashith, G. K. Roa, and G. Sanjeev, *Ceramics. International*, **43**: 10487 (2017); https://doi.org/10.1016/j.ceramint.2017.05.094
12. M. C. Lopez, J. P. Espinos, F. Martin, D. Leinen, and J. R. Ramos-Barrado, *Journal of Crystal Growth*, **285**, Iss. 1–2: 66 (2005); https://doi.org/10.1016/j.jcrysgro.2005.07.050
13. S. Mondal, S. Bhattacharyya and P. Mitra, *Pramana*, **80**, Iss. 2: 315 (2013); https://doi.org/10.1007/s12043-012-0463-6
14. C. F. Niedik, C. Freye, F. Jenau, D. Haring, G. Schroder, and J. Bittmann, *2016 IEEE International Conference on Dielectrics (ICD)*, **2**: 1114 (2016); https://doi.org/10.1109/ICD.2016.7547814
15. X. Huang, N. Hu, L. Zhang, L. Wei, H. Wei, and Y. Zhang, *Synthetic Metals*, **185**: 25 (2013); https://doi.org/10.1016/j.synthmet.2013.09.034
16. H. Wu, J. Yu, G. Yao, Z. Li, W. Zou, X. Li, and Z. Tang, *Sensors and Actuators. B: Chemical*, **369**: 132195 (2022); https://doi.org/10.1016/j.snb.2015.01.070